Final Draft
of the original manuscript:

Dieringa, H.; Hort, N.; Kainer, K.U.:

Investigation of minimum creep rates and stress exponents calculated from tensile and compressive creep data of magnesium alloy AE42

In: Materials Science and Engineering A (2008) Elsevier

DOI: 10.1016/j.msea.2008.06.051

Investigation of minimum creep rates and stress exponents calculated from tensile and compressive creep data of magnesium alloy AE42

Hajo Dieringa*, Norbert Hort, Karl Ulrich Kainer
GKSS Research Centre, MagIC – Magnesium Innovation Centre,
Max-Planck-Str. 1, 21502 Geesthacht, Germany

Key words: Magnesium, AE42, tension, compression, creep, threshold stress, twinning

Abstract

Creep specimens prepared of magnesium alloy AE42 were investigated under constant load in compressive and tensile creep respectively. Material was cast via the squeeze casting process in order to obtain a dense microstructure without pores. Creep tests were performed at constant temperatures between 150°C and 240°C and constant applied stresses between 40 MPa and 120 MPa until minimum creep rate $\dot{\varepsilon}_s$ was reached. It could be seen that the minimum creep rates of compressive creep tests were smaller compared to tensile creep tests, and the difference increased with increasing applied stress. Stress exponents, n, were determined according to the Norton-equation and it was found that a threshold stress σ_0 had to be introduced into the analysis. The threshold stress is based on strengthening by Al-RE (aluminum-rare earths) precipitates. Calculating the true stress exponent, n_t, deformation mechanisms during creep could be clarified.

Introduction

The increasing interest in magnesium alloys for automotive applications is the consequence of the need to reduce the weight of cars in order to save fuel and reduce emission of carbon dioxide. Use of magnesium alloys reached a maximum in the 1930´s and 1940´s, but after

* Corresponding author. Tel: 0049(+)4152-871955; fax: 0049(+)4152-87-1909; E-mail address: hajo.dieringa@gkss.de

WW2 the production decreased significantly. The recent increase started in the early 1990´s. Recent efforts have been made to improve creep resistance. Either the reduction of aluminum combined with the addition of elements that preferentially combine with aluminum, or the complete elimination of aluminum as an alloying element were taken into account. The need to eliminate or reduce the aluminum content is because β-phase ($Mg_{17}Al_{12}$) contributes to the poor creep resistance in aluminum containing Mg-alloys [1]. Concerning the aluminum containing magnesium high-pressure-die-cast (HPDC) alloys, AE42 currently shows very good creep properties. This is due to the Al-RE precipitates, which suppresses the formation of $Mg_{17}Al_{12}$ [2, 3]. It is well known that creep resistance plays an important role concerning the long term stability of castings. Usually creep tests are performed in tension, but real loading conditions are often compressive. For example, bolting of magnesium gearbox housings or engine parts results in a compressive stress on the castings.

Casting of the material

The squeeze cast process [4-6] was used for production of the material. The slow filling of the die, which occurs without a turbulent stream of the melt, causes a porefree microstructure of the castings. Another reason for the optimum microstructure is solidification under pressure. During the casting process the die has a temperature of 300°C at the sides and 150°C at the bottom. The superheated melt, with a temperature of 770°C, is poured into the die manually, and a ram squeezes the melt into the die with a speed of 10 mm/s. The solidification pressure is 100 MPa which is maintained for 20 s. The direct squeeze casting process works without a gate system. The upper ram is part of the die, so the amount of melt is directly proportional to the size of the casting. Figure 1 shows a sketch of the squeeze casting process.

The magnesium alloy AE42 contains aluminum and rare earth elements as main alloying elements. For a more precise analysis spark excited optical emission spectroscopy was done. Table 1 shows the composition of the alloy AE42.

Creep tests

Usually lightweight alloys are loaded in compression (e.g. bolt areas of gear box housings or engines). Creep tests are usually performed in tension. Cylinders with a diameter of 6 mm and a length of 15 mm were prepared by spark erosion technique for compression tests. Specimens with a gauge length of 30 mm, a diameter of 6 mm and M10 threads were turned for tensile creep tests. The creep tests were performed at ATS Lever Arm Test Systems under constant stress between 40 MPa and 120 MPa and temperatures of 150°C, 175°C, 200°C and 240°C. Tests were performed until the specimen broke or until the minimum creep rate was reached. Figure 2 shows typical creep curves of tests performed in tensile and compressive mode at 175°C and 70 MPa.

Usually the dependence of minimum creep rate on applied stress is described by the Norton equation. It is given in (Eq. 1):

$$\dot{\varepsilon}_s = \frac{ADGb}{kT}\left(\frac{\sigma}{G}\right)^n \qquad \textbf{(Eq. 1)}$$

Where $\dot{\varepsilon}_s$ is the minimum or secondary creep rate, A is a dimensionless constant factor depending on the material, D the diffusion coefficient ($=D_0 \exp(-Q_c/RT)$ with D_0 the frequency factor, Q_c the activation energy for creep, R the gas constant and T the absolute temperature), G the shear modulus, b the Burgers vector and k the Boltzmann constant. In order to evaluate stress exponent, n, the slope of a plot of log $\dot{\varepsilon}_s$ against log σ has to be evaluated. Plots for creep tests performed at 150°C, 175°C, 200°C and 240°C are shown in Figures 3 a-d, respectively. Values of stress exponents are inserted in the plots.

Stress exponent n is directly related to deformation mechanisms taking place during creep. A value of n = 3 is related to viscous glide of dislocations [7-9], n = 5 is related to dislocation climbing at high temperatures [7, 8, 10] and n = 7 to dislocation climbing at low temperatures [11]. A value of n = 1 is connected to diffusion deformation mechanisms [12, 13].

For magnesium alloy AS21, similar creep tests in tension have been performed [14]. It can be seen that stress exponents, especially in tensile creep tests, are very high compared to

theoretical values. It is not possible to explain deformation mechanisms occurring during creep with those stress exponents directly. High stress exponents are often identified in creep tests with dispersion strengthened materials or metal matrix composites. AE42 based MMC reinforced with 20 vol.-% Saffil-fibres was investigated recently [15]. They are explained with the appearance of a threshold stress σ_0, which reduces the applied stress σ and is connected to phenomena of interaction between obstacles and dislocations. Three explanations can be found in metallic materials:

- Threshold stress is the stress which is needed to bow a dislocation between two obstacles [16-18], corresponding to the Orowan stress.
- Threshold stress corresponds to an additional back stress which is built up during climbing over an obstacle, and is needed to elongate the dislocation [19].
- Threshold stress corresponds to an additional stress which is needed after climbing over an obstacle to detach from it [20, 21].

Li and Langdon developed a method to calculate the threshold stress [22]. They assumed that a minimum creep rate of 10^{-10} s^{-1} is the lowest rate that is conveniently measurable in creep experiments. In the double logarithmic plots of minimum creep rate against applied stress, an extrapolation of the fitted lines to a value of 10^{-10} s^{-1} gives the stress value which is assumed to be the threshold stress. Carrying out this procedure, threshold stresses were found which are shown in Figure 4. Threshold stresses calculated from compression creep tests are approximately 10 MPa lower than those found in tensile creep tests.

Introducing threshold stresses, (Eq. 1) changes into (Eq. 2):

$$\dot{\varepsilon}_s = \frac{ADGb}{kT}\left(\frac{\sigma-\sigma_0}{G}\right)^{n_t} \qquad \textbf{(Eq. 2)}$$

For calculation of the true stress exponent n_t double logarithmic plots of $(\sigma-\sigma_0)$ against minimum creep rate have to be made. Figures 5 a-d show these plots. The values of n_t are inserted in the plots. True stress exponents found in compression creep tests are always lower than exponents found in tensile tests. According to the evaluated values of n_t both

compressive and tensile deformation occurs by glide. At higher temperatures climb of dislocations also occurs.

Optical microscopy

Figure 6 shows an optical micrograph of AE42 in the as cast state. Magnesium alloy AE42 manufactured via squeeze casting with a relatively slow solidification (compared to die casting) shows a dendrite structure with lamellar precipitates of $Al_{11}RE_3$, Al_4RE and Al_2RE and spherical precipitates of $Al_{10}RE_2Mn_7$. The latter phase is marked with A and the AlRE phases are marked with B.

Figures 7 a-c show the microstructure after creep at a temperature of 200°C and stresses of 40, 60 and 80 MPa, respectively, for compression (left graph) and for tension (right graph). After 40 MPa tests there is no change in microstructure compared to the as-cast state, whereas after tests at higher stresses, twinning occurs. During compression creep, twinning occurs only in one direction (primary twinning) whereas in tension there is also secondary twinning observable.

Conclusions

Creep tests in compressive and tensile mode were performed under constant stresses between 40 MPa and 120 MPa at constant temperatures of 150°C, 175°C, 200°C and 240°C until the specimen failed or reached the minimum creep rate. Following the Norton equation, stress exponents were calculated, and it was found that, especially the tension, stress exponents are very high compared to theoretical values and deformation mechanisms are not related to experimental stress exponents. By introducing a threshold stress, as is common for dispersion strengthened metals or composites and has been shown for magnesium alloy AS21 already [14], values of true stress exponents are found to be suitable for determination of mechanisms which occur during creep. Gliding and climbing of dislocations are the predominant deformation mechanisms. Microstructure investigations using optical microscopy have shown

that at low stresses, where no twinning occurs, minimum creep rates of tensile and compressive creep tests are very similar. At increasing stresses minimum creep rates diverge. It can be seen in Figures 7 b and c that during compressive creep primary twins and during tensile creep primary and secondary twins appear. The differences in the minimum creep rates can be attributed to the different twinning behaviour. Additional secondary twinning results in additional areas in which dislocations can glide easily.

Literature

[1] W. Blum, P. Zhang, B. Watzinger, B. V. Grossmann, H. G. Haldenwanger, Mater. Sci. Eng. A319-32 (2001) 735-740.
[2] B.R. Powell, V. Rezhets, M.P. Balogh, R.A. Waldo, JOM 54 (2002) 34-38.
[3] Y. Fasoyinu, M. Sahoo, C.J. Bettles, G. Prior, Proc. 1st Int Light Metals Techn. Conf. 2002 A. Dahle (Ed.) (2002) 137-142.
[4] K.U. Kainer, E. Böhm, VDI-Berichte **1235** (1995) 117-125.
[5] G.A. Chadwick, Mat. Sc. Eng. **135A** (1991) 23-28.
[6] H. Hu, J. Mat. Sc. **33** (1998) 1579-1589.
[7] O.D. Sherby, P.M. Burke, Progress in Mater. Sc. **13** (1968) 325-389.
[8] F.A. Mohamed, K.T. Park, E.J. Lavernia, Mat. Sc. Engin. **A150** (1992) 21-35.
[9] J. Weertman, J. Appl. Phys. **28** 3 (1957) 362-364.
[10] J. Weertman, J. Appl. Phys. **28** 4 (1957) 1185-1189.
[11] S.L. Robinson, O.D. Sherby, Acta Met. **17** (1969) 109-125.
[12] J. Harper, J.E. Dorn, Acta Met. **5** (1957) 654-665.
[13] A.J. Ardell, S.S. Lee, Acta Met. **34** (1986) 2411-2423.
[14] P.Zhang, Scr. Mat. **52** (2005) 277-282.
[15] H. Dieringa, Y. Huang, P. Maier, N. Hort, K.U. Kainer, Mat. Sci. Eng. **410-411** (2005) 85-88.
[16] W.C. Olliver, W.D. Nix, Acta Metall. **30** (1982) 1335-1339.
[17] E. Orowan, in: M. Cohen (Ed.) Dislocation in Metals, AIME, New York (1954) 131.
[18] U.F. Kocks, Phil. Mag. **13** (1966) 541.
[19] E. Arzt, M.F. Ashby, Scr. Metall. **16** (1982) 1285-1290.
[20] E. Arzt, D.S. Wilkinson, Acta Metall. **34** (1986) 1893-1898.
[21] E. Arzt, J. Rösler, Acta Metall. **36** (1988) 1053-1060.
[22] Y. Li, T.G. Langdon, Scr. Mater. **36** 12 (1997) 1457-1460.

Table 1: Composition of alloy AE42

Element	Al	Mn	Si	Ce	La	Nd	Pr	Th	Mg
wt.-%	3.9	0.3	0.01	1.2	0.6	0.4	0.1	0.2	rem.

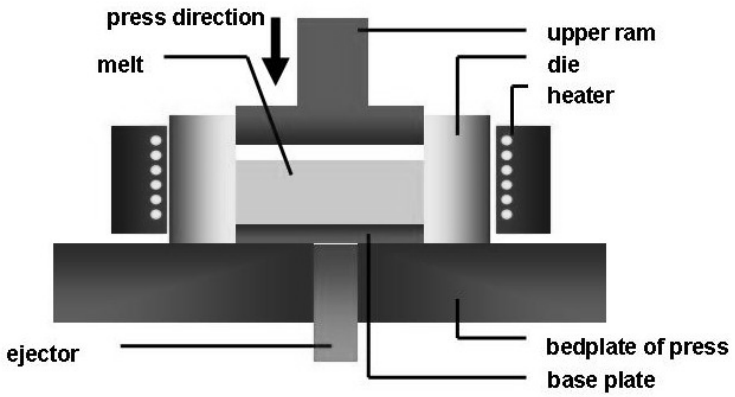

Fig. 1: Sketch of a squeeze casting tool.

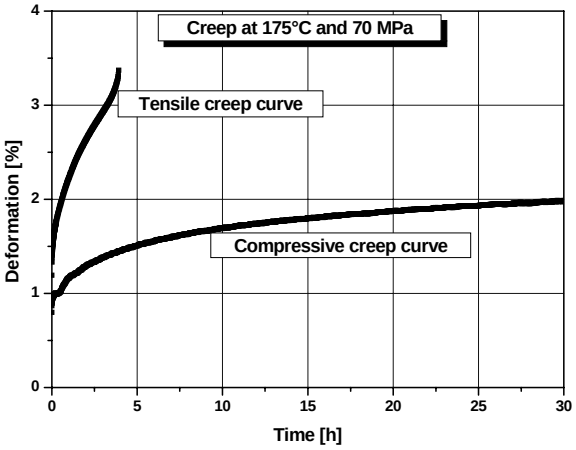

Fig. 2: Tensile and compressive creep curves (175°C and 70 MPa).

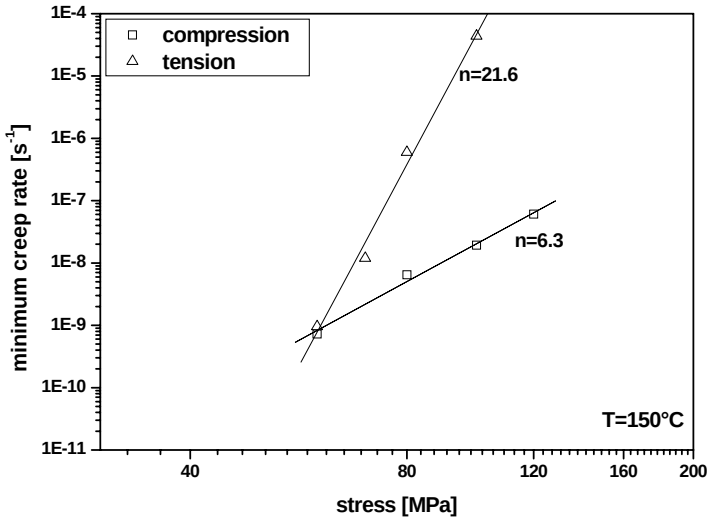

Fig. 3a: Norton-plots of tests performed at 150°C.

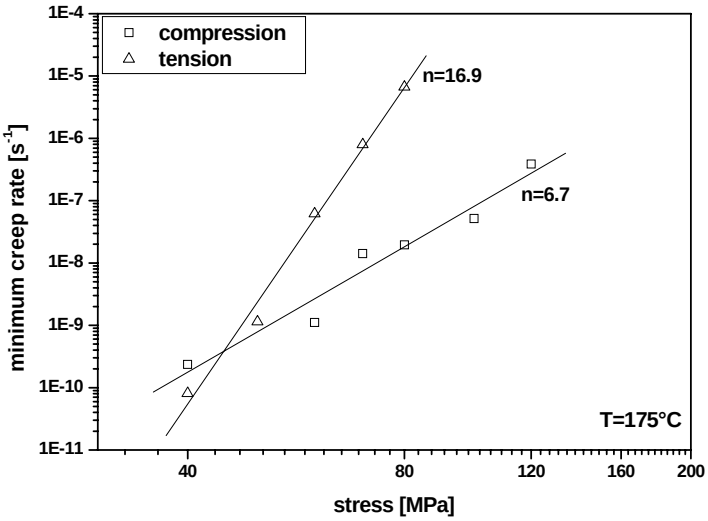

Fig 3b: Norton plots of tests performed at 175°C.

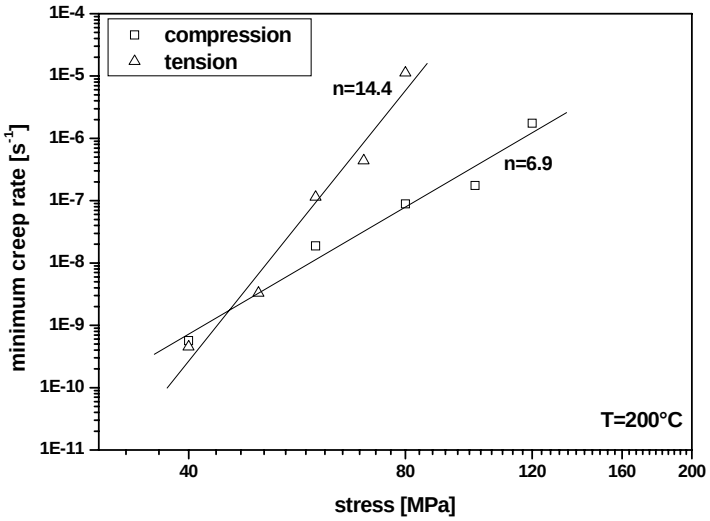

Fig. 3c: Norton-plots of tests performed at 200°C.

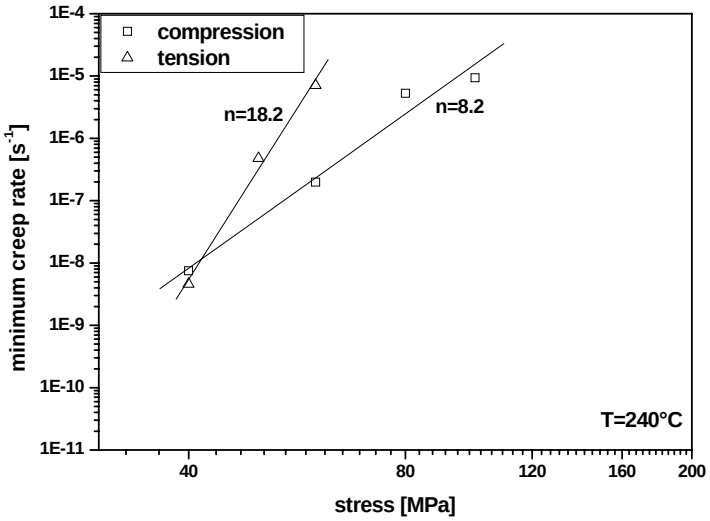

Fig. 3d: Norton-plots of tests performed at 240°C.

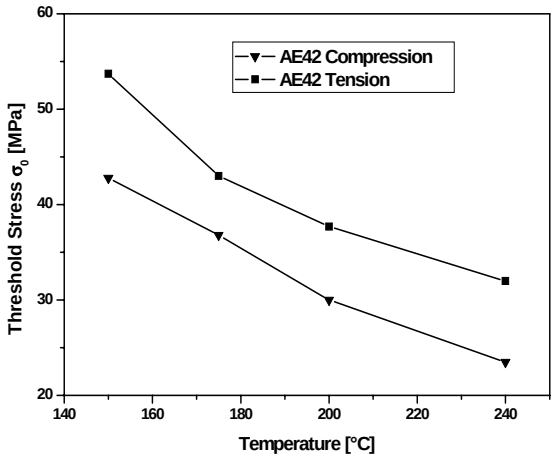

Fig. 4: Threshold stresses calculated with method from Li et al. [22].

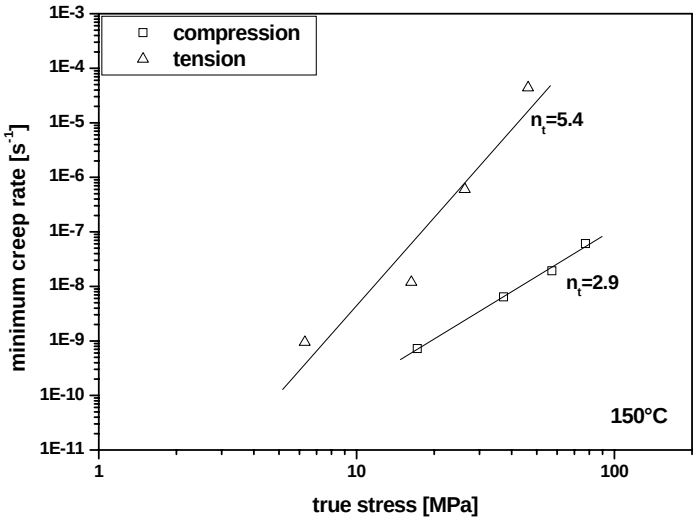

Fig. 5a: Plots of (σ-σ_0) against $\dot{\varepsilon}_s$ at 150°C.

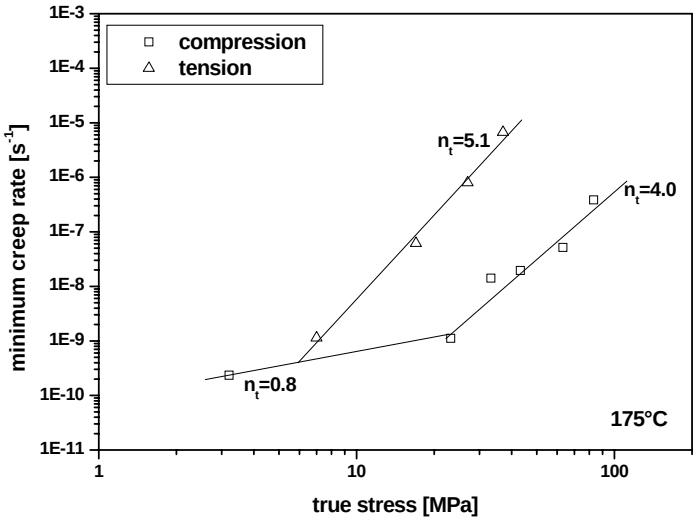

Fig. 5b: Plots of $(\sigma-\sigma_0)$ against $\dot{\varepsilon}_s$ at 175°C.

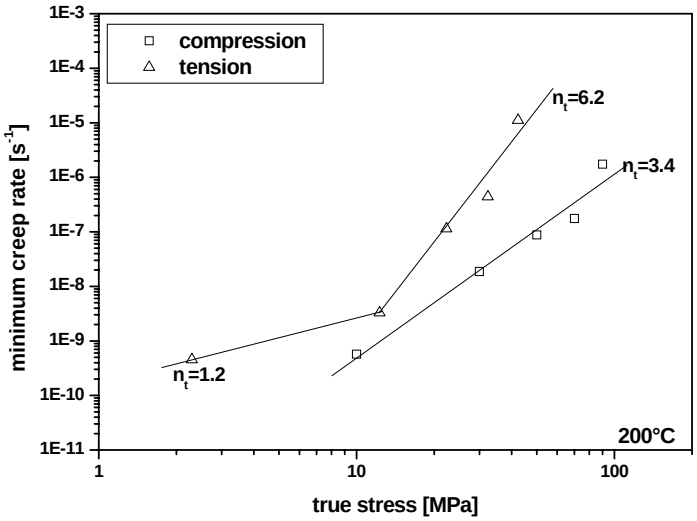

Fig. 5c: Plots of (σ-σ_0) against $\dot{\varepsilon}_s$ at 200°C.

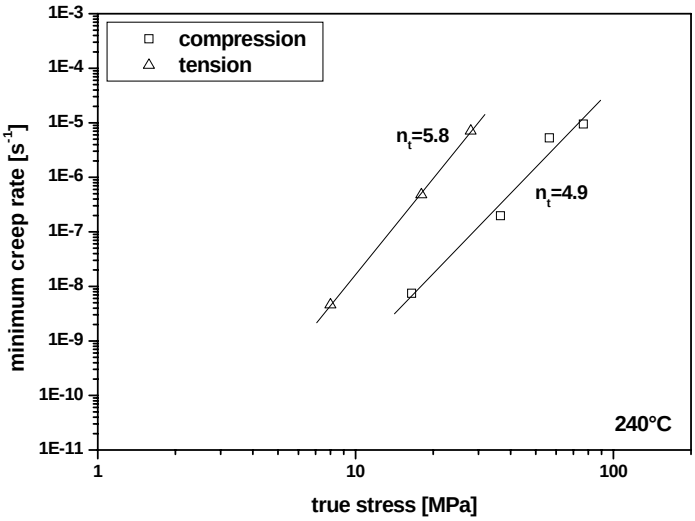

Fig. 5d: Plots of (σ-σ_0) against $\dot{\varepsilon}_s$ at 240°C.

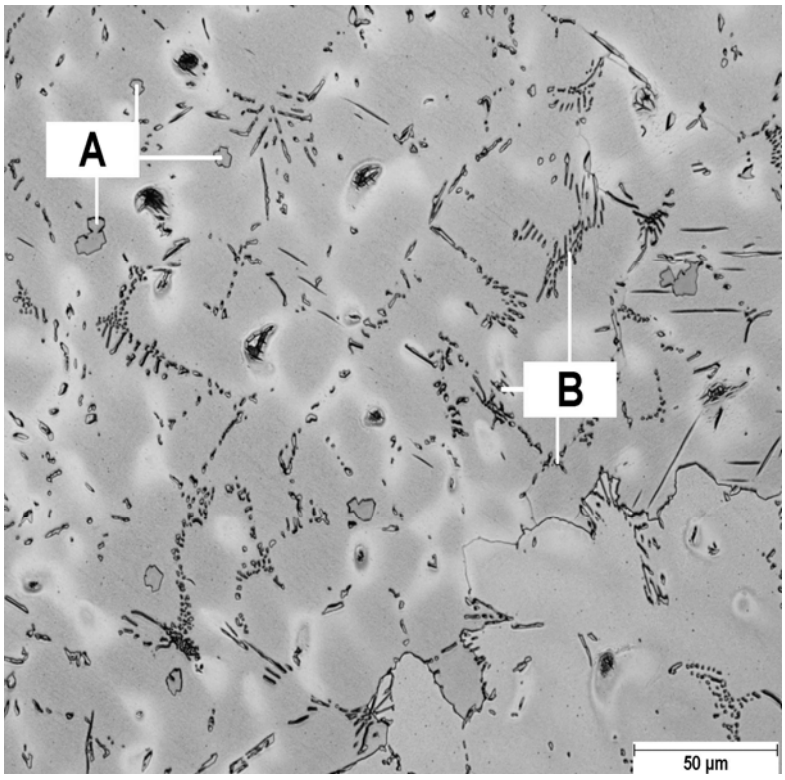

Fig. 6: Microstructure of AE42 in the as cast state.

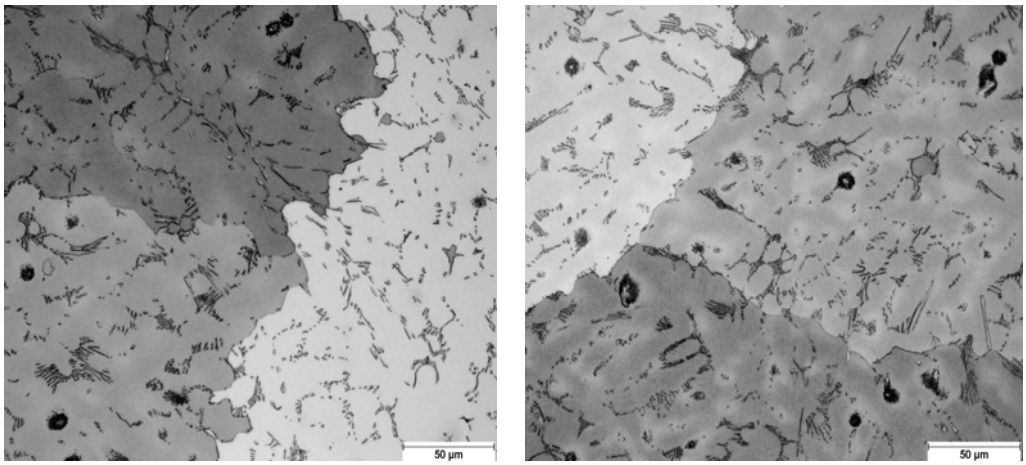

Fig. 7a: Microstructure after creep at 200°C and 40 MPa; left: compression, right: tension.

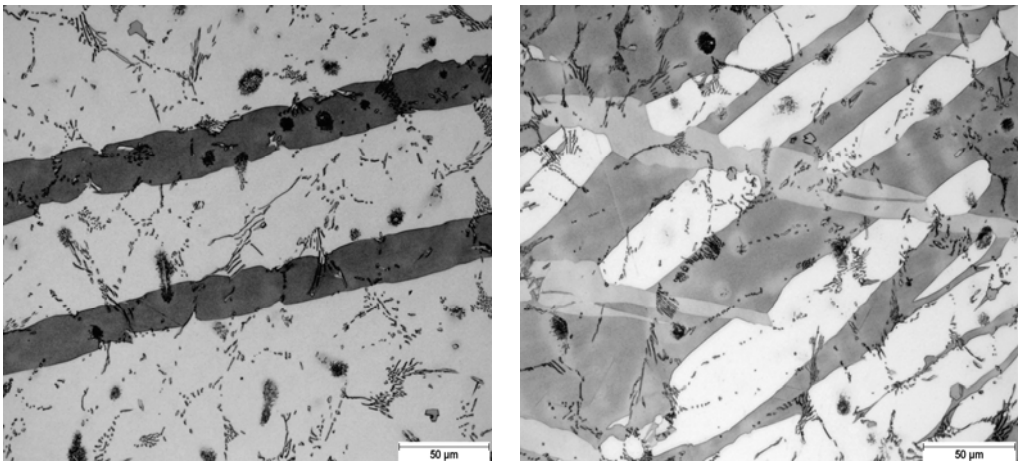

Fig. 8b: Microstructure after creep at 200°C and 60 MPa, left: compression, right: tension.

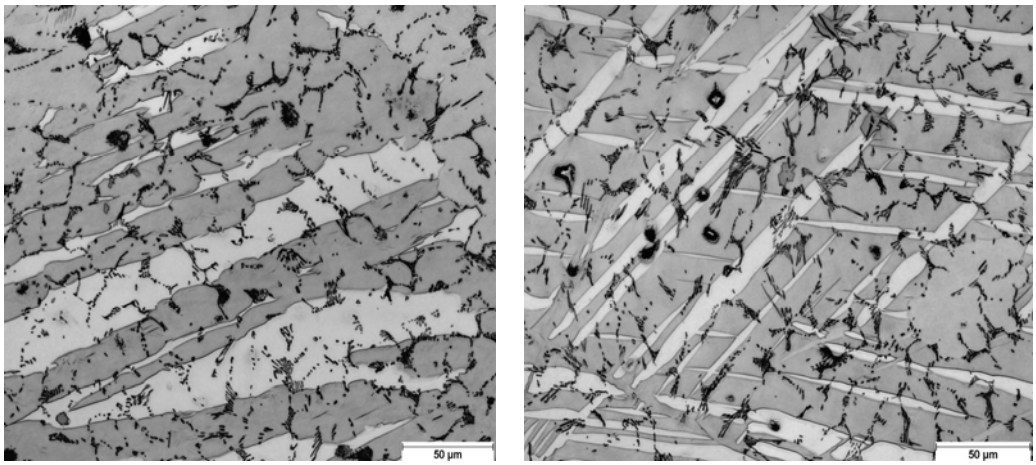

Fig. 8c: Microstructure after creep at 200°C and 80 MPa; left: compression, right: tension: